



ChemTech

International Journal of ChemTech Research

CODEN (USA): IJCRGG, ISSN: 0974-4290, ISSN(Online):2455-9555
Vol.9, No.12, pp 647-655, 2016

Complex Dynamics of QD Light Emitting Diode with Optoelectronic Feedback

RaheemA. Jebara

Engineering College, University of Thi-Qar, Nasiriyah, Iraq

Abstract : We studied a three-variable dimensionless model for a quantum dot light emitting diode (QDLED) subject to optoelectronic feedback. In dependence of the feedback strength and delay-time we analyze complex bifurcation scenarios for the intensity of the emitted light as well as time series, FFT and phase plane of all dynamic variables in order to elucidate the internal dynamics of the light emitting diode. Furthermore, the chaotic dynamics is completely determined by both the variation of the optoelectronic feedback strength and delay-time of the QDLED, as evidenced by bifurcation diagram. Our results showed that small feedback strength lead to lower sensitivity of the light emitting towards optoelectronic feedback.

Keywords : quantum-dot light emitting diode, optoelectronic feedback, FFT, chaos, control.

Introduction

Irregular spiking sequences in biological, chemical and electronic systems have been frequently observed to be the result of multiple timescale dynamics¹. Indeed, a variety of natural systems showing this behavior (neural cells², cardiac tissues³, chemical reactions⁴, to name just a few) can be mathematically described by means of slow and fast variables coupled together (slow-fast systems). In order to understand these complex dynamics, frequently observed in biological environments, and to provide controllable and reproducible experiments, considerable efforts have been devoted to the search for analogous phenomena in nonlinear optical systems, and homoclinic chaos has been found in lasers with feedback⁵ and with a saturable absorber⁶.

Optoelectronic feedback is one of the perturbations to the injection current in QDLED that induces instabilities. In optical feedback to QDLEDs, the phase sensitivity plays a crucial role in the QDLED dynamics⁷. However, different from optical feedback, we do not need to consider the phase effect in optoelectronic feedback systems, since the phase information is once eliminated by a photodetection in the feedback process⁸. Stable or unstable operations of lasers are flexibly and reliably controlled through the injection current^{9,10}. The dynamics of QDLED with optoelectronic feedback can be described only by the three equations of the photon number and carrier number in dot and wetting region. Therefore, optoelectronic feedback shows different dynamics from those of optical feedback in QDLEDs.

For optoelectronic feedback through the injection current, there are two categories; one is positive feedback and the other negative feedback. They have different mechanisms for driving the dynamics of the output. In negative feedback, the feedback current is deducted from the bias injection current and it induces the sharpening of the relaxation oscillation¹¹.

On the other hand, the feedback current is added to the bias injection current and, as a result, the delay-time varying tends to drive the output into pulsing states. In this study we present a rate-equation analysis which incorporates the essential aspects of electronic transitions. We apply the analysis to propose a rate equations model of three levels states in dimensionless form that exhibits extremely complicated behaviors and modulation rate of QDLEDs, taking into account both the photon reabsorption and nonradiative recombination processes. The paper is organized as follows: after introducing our model approach in Section II then in Section III with the optoelectronic feedback modes, we will study the bifurcation scenarios of the light emitting output that occur by changing the feedback strength and delay-time. The impact of the parameters variation of light emitting instability will be discussed. In Section IV.

I. QDLED model

We shall study QD LED structures using rate equations. In the QD LED system the electrons are first injected into the wetting layer WL before they are captured by the QDs. We consider a system made up of upper electronic levels, and lower electronic levels. The equations describe the dynamics of the total number n_{QD} of carriers in the upper levels, n_{wl} number of carriers in the WL, and the number of photons in the optical mode S , as follows:

$$\begin{aligned} \dot{S} &= An_{QD} - dS - \gamma_s S, \\ \dot{n}_{QD} &= \gamma_c n_{wl} \left(1 - \frac{n_{QD}}{2Nd} \right) - \gamma_r n_{QD} - (An_{QD} - dS), \\ \dot{n}_{wl} &= \frac{J}{e} - \gamma_n n_{wl} - \gamma_c n_{wl} \left(1 - \frac{n_{QD}}{2Nd} \right) \end{aligned} \quad (1)$$

here, A is the spontaneous emission rate into the optical mode, γ_r and γ_n are the non-radiative decay rates of the number of carriers in the upper levels and WL respectively; N_d is the total number of QDs; and J is the injection current, e is elementary charge, γ_c is the capture rate from WL into an empty dot, and d and γ_s are the absorption and output coupling rate of photons in the optical mode, respectively.

For a three-level atomic system where the transition is homogeneously broadened, it can be shown from the Einstein relation that¹²

$$d = \Gamma A n_o \quad (2)$$

Where n_o the occupation number of the lower level and \tilde{A} is the confinement factor. In such a case, the spontaneous emission coefficient and absorption coefficient possess identical lineshapes. For realistic material systems, such as semiconductor or organic emitters, both the lower and the upper levels can be inhomogeneously broadened. Population distributions in the lower and upper levels have to be taken into account explicitly in order to determine the correct relation between absorption and spontaneous emission spectra¹³. The energy scheme of the QDLED is shown in Fig.1.

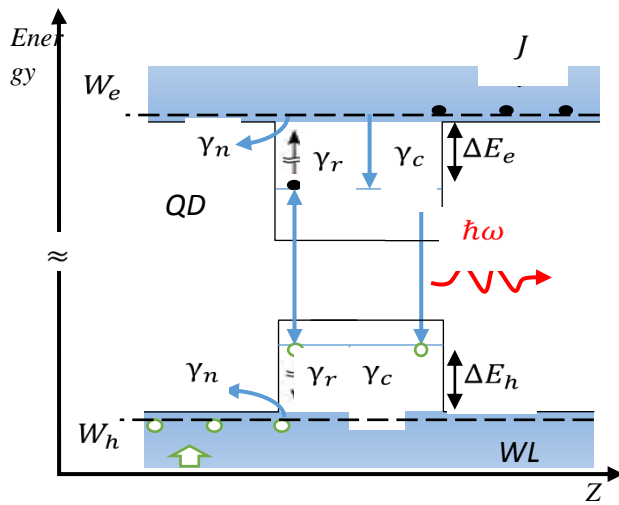


Figure .1 Energy diagram illustrating of the two recombination mechanisms considered in this work of the active layer QD LED; recombination radiative and non-radiative via deep level and reabsorption recombination processes.

The main goal of this work is to provide a physical model reproducing qualitatively the experimental results and showing that irregular spiking sequences is the result of the optoelectronic feedback of the QDLED. Applying optoelectronic feedback to QDLEDs induces a dramatic change in the photon statistics wherein strong, super-thermal photon bunching is indicative of random intensity fluctuations associated with the spike emission of light, as will be reported in this work. To do so, we rescale the system (1) to a set of dimensionless equations as is done more often in the literature¹⁴⁻¹⁶. Defining new variables and dimensionless parameters by

$$x = S, \quad y = \frac{A}{\gamma_s}(n_{QD} - n_o S),$$

$$w = \frac{n_{wl}\gamma_c}{A}, \quad \gamma_n = \frac{t'}{t},$$

$$\gamma = \frac{\gamma_s}{\gamma_n}, \quad \gamma_1 = \frac{A}{\gamma_n}, \quad \gamma_2 = \frac{A}{\gamma_s},$$

$$\gamma_3 = \frac{\gamma_r}{\gamma_n}, \quad \gamma_4 = \frac{\gamma_c}{\gamma_n},$$

$$N_d \equiv a, \quad n_o \equiv b \text{ and } \delta_o = \frac{J}{Ae}$$

Eqs. (1) can be rewritten in the following form

$$\dot{x} = \gamma(y - x),$$

$$\dot{y} = \gamma_1 \gamma_2 w \left(1 - \frac{b}{a} x\right) - \gamma_1 y \left(1 + \frac{1}{a} w\right) - b \gamma_1 (x - y) - \gamma_3 (y + \gamma_2 x),$$

$$\dot{w} = \gamma_4 \delta_o - w \left(1 - \frac{\gamma_4}{a \gamma_2} y\right) - \gamma_4 w \left(1 - \frac{b}{a} x\right) \quad (3)$$

Here, prime means differentiation with respect to t and the bias current is represented by δ_o .

II. QDLED model with Optoelectronic feedback

The model of optoelectronic feedback in QD-LEDs is the same as that treated as the direct current modulation discussed in our recently works. Fig.2 shows a schematic diagram of optoelectronic feedback in a QDLED. The light emitted from a QDLED is detected by a photodiode and the detected photocurrent is fed back through a bias Tee circuit. The feedback may be positive or negative depending on the polarity of the output of the amplifier in the circuit. In optoelectronic feedback, the modulation is not for the complex field but for the population through the disturbance to the injection current. Therefore, we use the rate equation of the photon number instead of the complex amplitude. Using (1) and (3), the rate equations for the optoelectronic feedback system is written by

$$\begin{aligned}
 \dot{S} &= -dS - \gamma_s S + An \\
 \dot{n}_{QD} &= \gamma_c n_{wl} \left(1 - \frac{n_{QD}}{2N_d}\right) - \gamma_r n_{QD} - (An - dS) \\
 \dot{n}_{wl} &= \frac{J}{e} \left(1 + \frac{k S(t - \tau)}{S_o}\right) - \gamma_n n_{wl} - \gamma_c n_{wl} \left(1 - \frac{n_{QD}}{2N_d}\right)
 \end{aligned} \quad (4)$$

Where k is the feedback strength. The system is positive feedback for a positive value of k , while it is negative feedback for a negative value. S_o is the steady state value for the photon number. δ is the feedback time including time responses of the detector and the electronic circuits.

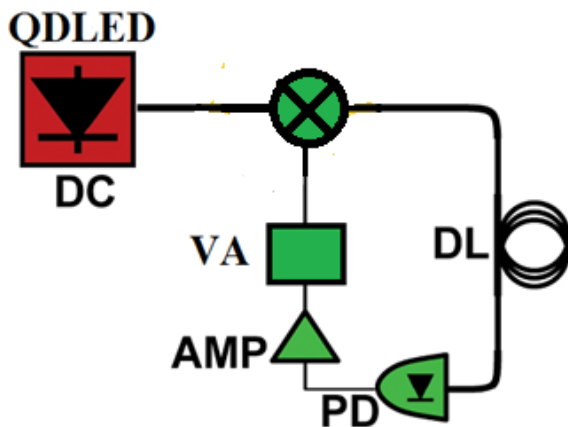


Figure. 2. Schematic diagram of the optoelectronic feedback system. QDLED: quantum dot light emitting diode; PD: Photodiode; AMP: amplifier; VA: variable attenuator; DL: Optical delay line. Nonlinearity due to the maxing it is external to the output.

The output light is received and converted to a current by a photodiode which it is proportional to the optical intensity. The current is subsequently amplified and added to the bias current, resulting in a delayed positive feedback. The delay time can be varied by changing the distance between the QDLED and the photodiode. In our numerical investigations of the delay differential equations, which describe the dynamics of the optoelectronic feedback QDLED, we find a rich bifurcation diagram as the delay time and the feedback strength are varied. In general chaotic regions are interspersed with periodic and quasi-periodic ones and multistability of different types of attractors, e.g. fixed points and limit cycles, are a common feature. We find that the optoelectronic feedback QDLED enters chaos through the quasi-periodic route. This agrees well with results from analytic bifurcation analyses of the delay differential equations modeling the system. The parameter values used in the simulations are given in Table (1).

Table. 1 Numerical parameters used in the simulation unless stated otherwise.

Parameters	value	Parameters	value
x_o	0.066	γ_2	0.03
y_o	0.99	γ_3	0.07
w_o	0.0049	γ_4	0.087
γ	0.172	a	1.04
γ_1	0.144	b	3.838

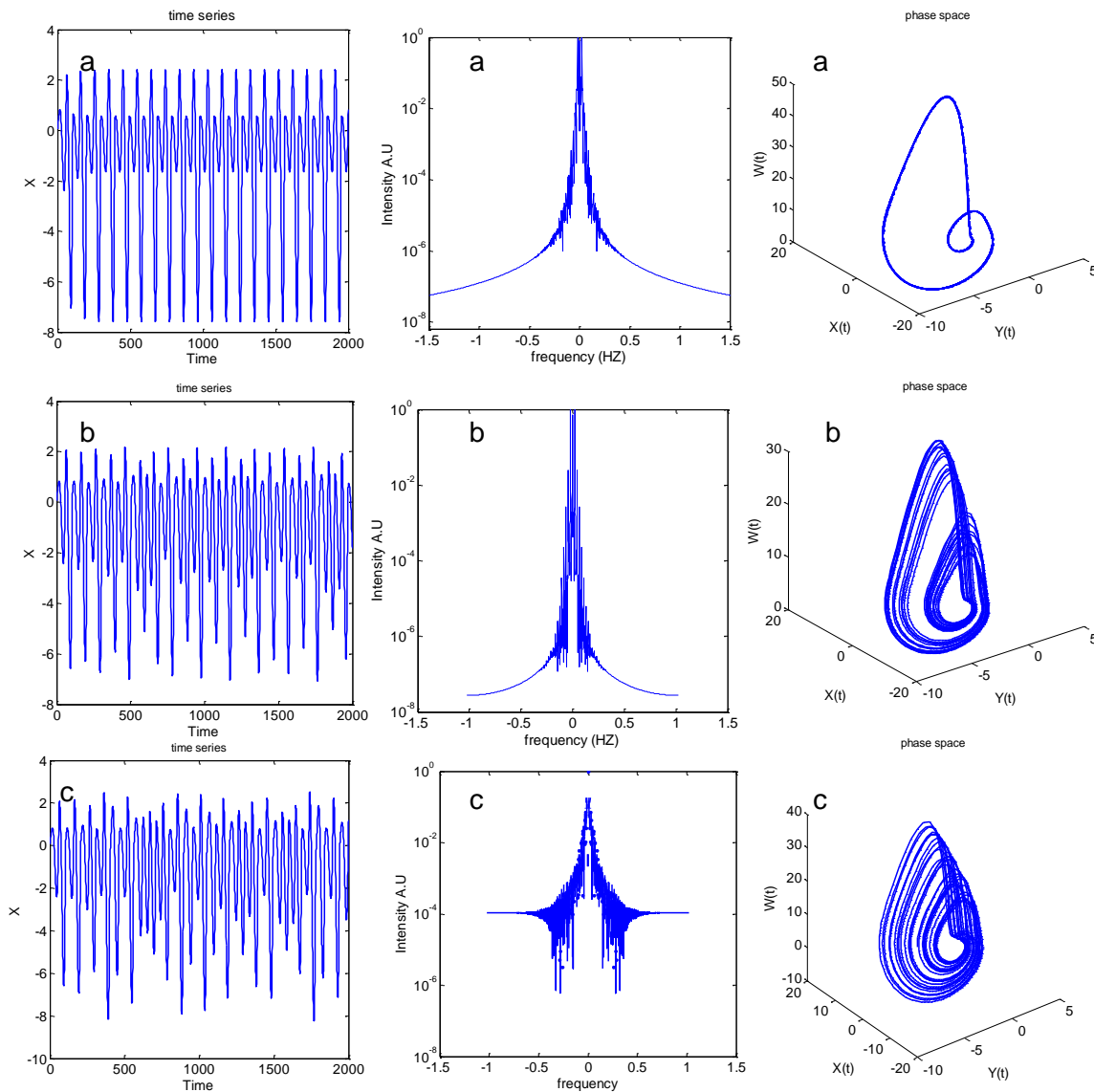


Figure 3. Theoretically results: time series, FFT and attractor sections at different delay times. From top to bottom: (a) periodic oscillations, at $\hat{\delta} = 10$; (b) two-frequency quasi-periodicity, at $\hat{\delta} = 49.5$; (c) chaos, at $\hat{\delta} = 55$. The broadband background in (c) is much higher than in (b), indicated by the reference lines at 10^{-7} (a.u). The parameters measured are $\hat{a}_o = 1.6$ and $k = 0.2$.

Fig. 3 shows the theoretically observed time series of the QDLED output, the corresponding Fourier transformations of the output spectrum so-called fast Fourier transform (FFT), and the corresponding attractors at different time delays. The attractor is obtained in a delay-embedding space using the theoretical time series. The data shown in Figs. 3(a)-(c) were taken at measured delay times of $\hat{\delta} = 10, 49.5$ and 55 , respectively. The

time series in Figs. 3(a)-(c) show a clear transition from regular periodic oscillations to quasi-periodic oscillations with intensity amplitudes modulated at a certain second frequency, and finally to a chaotic state where the intensities vary irregularly. From the FFT, it is clear that in Fig. 3(a) there is only few fundamental frequency. The small ripples in the spectrum indicate that there is small instability in the QDLED. Then in Fig. 3(b), a more frequency, which corresponds to the increase of the delay time, is as significant of the frequencies in Figs. 3(a)-(b) are incommensurate and the system is in a two-frequency quasi-periodic oscillating state. Finally in Fig. 3(c), the spectrum is broadened as the system enters a chaotic pulsing state. Though some of the sharp spectral peaks remain in Fig. 3(c), the broadband background, a characteristic of chaos, is much higher in Fig. 3(c) than in Fig. 3(b), as indicated by the reference lines at 10^{-7} (a.u). The big cycle in the attractor section in Fig. 3(a) corresponds to regular periodic oscillations. The size of the cycle is an indication of the periodic in the data. Despite the periodic and the under-sampling the toroidal nature of the attractor for $\delta=49.5$ s can clearly be seen as a diffused closed curve in Fig. 3(b). In Fig. 3(c) the spread of the attractor plot indicates the transition to chaos.

Overall the numerical and experimental results show good agreement. The predicted quasi-periodic route to chaos is theoretically observed.

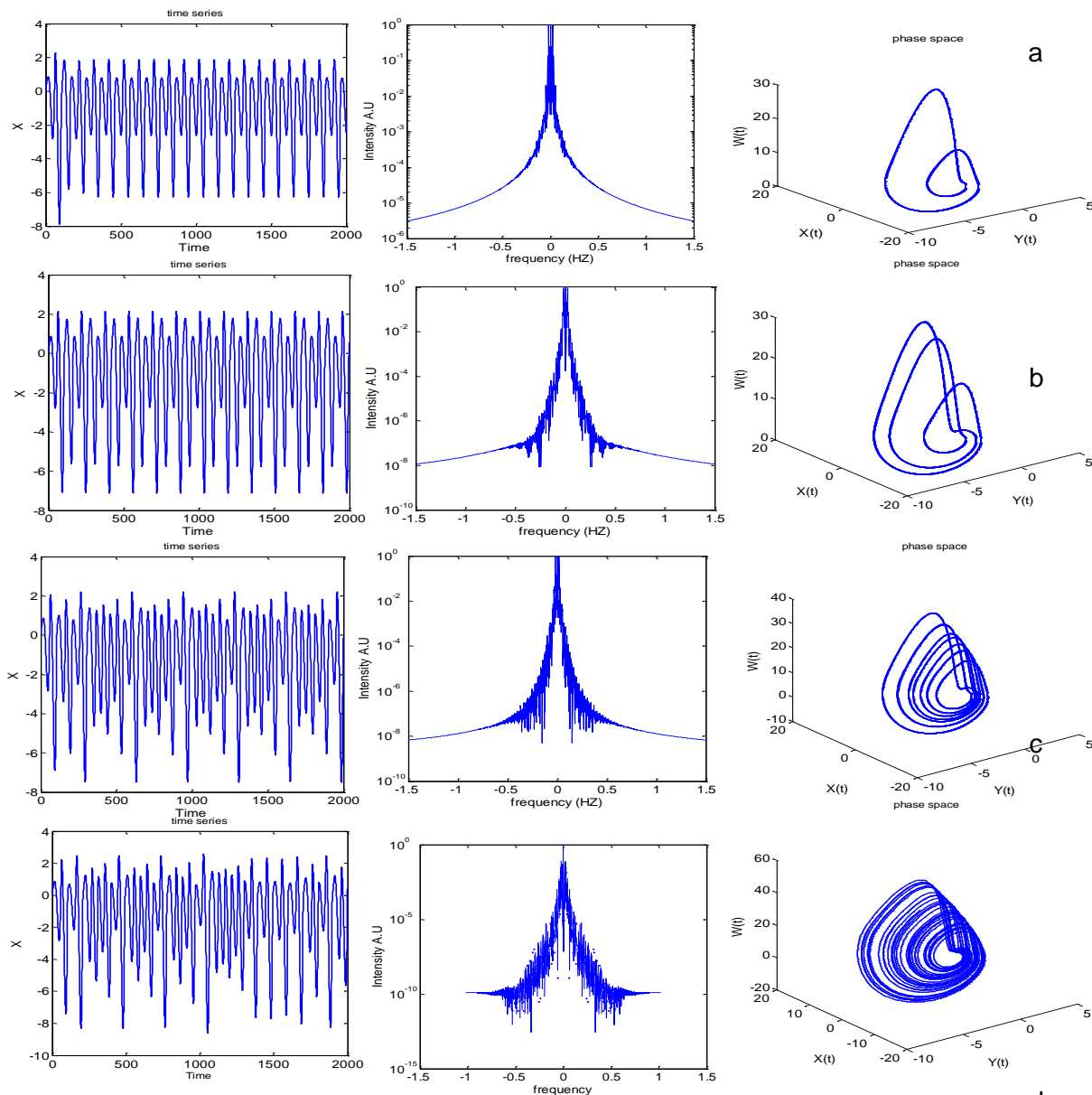


Figure 4. Time series, FFT and phase plane of different pulsing states. (a): regular periodic pulsing at $\hat{\delta}=60$. (b): more periodic pulsing at $\hat{\delta}=40$. (c): quasi-periodic pulsing at $\hat{\delta}=30$. (d): chaotic pulsing at $\hat{\delta}=27$. The calculated FFT have relative magnitudes with arbitrary unit. In the numerical simulations, the parameters are assumed to be $\ddot{a}_0=0.6$ and $k=0.2$.

Regular periodic pulsations are observed both for negative and positive optoelectronic feedback in QDLEDs. However, their dynamics are not always the same. For example, chaotic states are the typical feature in negative optoelectronic feedback, while they are rarely observed in positive optoelectronic feedback. The extent of chaotic regions in the parameter space varies. Here, we discuss chaotic evolutions of pulsing states in positive optoelectronic feedback systems and demonstrate that not only the pulse height but also the jitter of pulse sequences shows chaotic behaviors. Fig. 4 is a numerical result of pulsing states for the variations of the delay time in an optoelectronic feedback system (Eqs.4).

With $\hat{\delta} = 60$ in (a) of Fig. 4, the time series shows a sequence of regular periodic pulses with a constant pulsing intensity and interval. The corresponding FFT has few fundamental pulsing frequency, and attractor section in the last plane. When the delay time is decreased to $\hat{\delta} = 40$ in (b), the QDLED enters a more periodic pulsing state with the intensity modulated at an exponential frequency decay. The pulses are clearly observed in three cycles in the phase plane. When the delay time is further decreased to $\hat{\delta}=30$ in (c), the QDLED enters a quasi-periodic pulsing state as an extra exponential frequency and the phase plane is characterized by a torus. Finally, when $\hat{\delta} =27$, the QDLED enters a chaotic pulsing state as in (d), not only the pulse height but also the separation becomes chaotic (jitter) and the corresponding spectrum is much broadened. The phase plane spreads out over a wide range.

For a larger delay, the QDLED follows a quasi-periodic route into chaotic pulsing states. Fig. 5. (a) is the enlarged bifurcation diagram of a positive feedback strength and in Fig. 5.(b) denoted the negative feedback strength (a-d) in fig.4 can be compared with the pulsing states in Fig. 5. (a). The different pulsing states are indicated by the corresponding figures, where (a) is two frequency quasi-periodic pulsing, (b) is three-frequency quasi-periodic pulsing, (c) is quasi-chaotic pulsing and (d) is chaotic pulsing.

Fig.6 shows the bifurcation diagram of the photon density for (a) $\ddot{a}_o=0.6$ (b) $\ddot{a}_o=5.6$ as a function of the feedback strength. The bifurcation diagram in the figure are calculated numerically from Eq. (4). At first glance two striking differences can be seen compared to the ‘‘typical’’ QD LED case in Fig. 6(a) and (b) first, the sensitivity to the feedback is increased (the stable regions are much shorter) which results in a series of bifurcation cascades, and second, the direction of bifurcation solutions that are opposite to the QDLED is augmented by a type of mode.

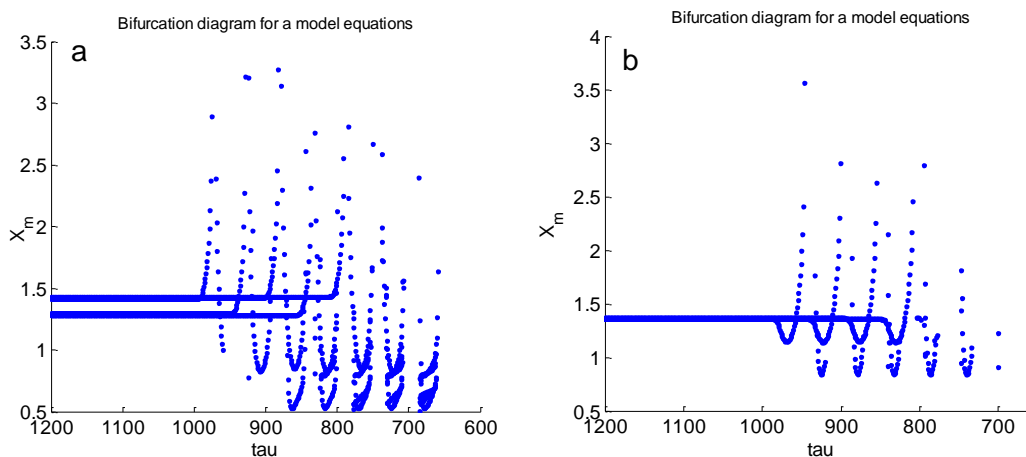


Figure. 5. Bifurcation diagram of extrema of peak series (a) negative feedback strength (b) positive feedback strength, with normalized delay time $\hat{\delta}$ varying inverse from 1200 to 600. Fig.4.(a) indicate the corresponding pulsing states, as in Fig. 4. In the numerical simulations, the parameters are assumed to be $\ddot{a}_o=5.6$ and $k=0.1$.

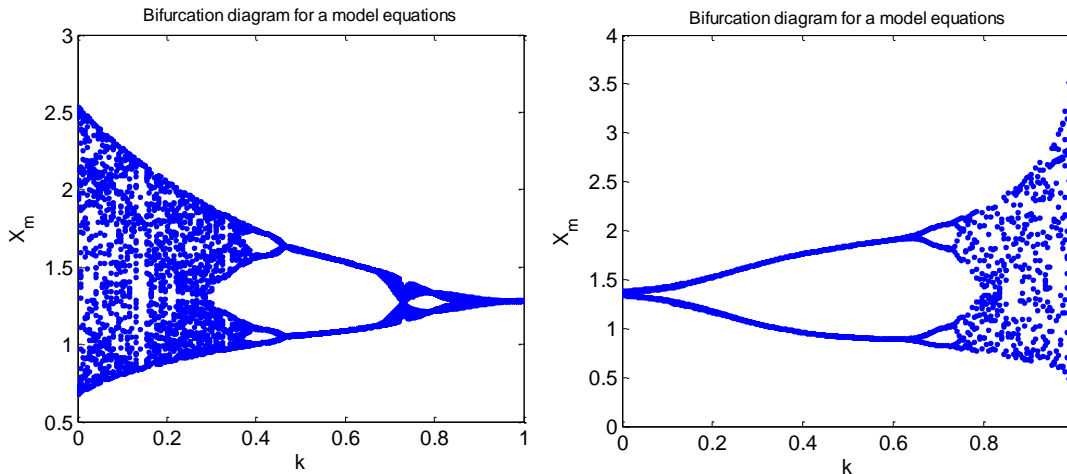


Figure. 6 Bifurcation diagrams of the photon density a (b) positive (negative) feedback mode in dependence of the feedback strength K for small value of $\ddot{a}_0=0.6$ (a) and another large $\ddot{a}_0=5.6$ (b) and delay time $\hat{o} =1500$.

III. Conclusion

In conclusion, we demonstrate that the existence of complex physical dynamics of a QDLED with coupled optoelectronic feedback loop. The rate equations model of this system is modified to dimensionless form and compute where its result show a transition from regular to irregular pulses. The transitions from periodicity to chaotic states by varying delay-time and fixing feedback strength have been noticed. The same behavior is achieved by fixing delay-time and varying feedback strength. But we could note here in both the positive and negative feedback strength that results are showed in a varying feedback strength case the dynamical behavior is opposite. The chaotic behavior could be studied in terms of FFT and attractor corresponding to time series, where chaotic happened at $\hat{o} = 27, 55$ and large 950 , and at $k = 0.3$ and 0.8 . We have studied several aspects of the dynamic response of excitable systems to different values of delay-time and feedback strength.

References

1. Jones C K and Khibnik A I 2000 Multiple-Time-Scale Dynamic Systems (IMA Proc. vol 122) (New York:Springer)
2. Izhikevich EM. (2000);Neural excitability, spiking and bursting. International Journal of Bifurcation and Chaos in Applied Sciences and Engineering. 10(6): 1171-1266.
3. Davidenko JM, Pertsov AV, Salomonsz R, Baxter W, Jalife J. (1992);Stationary and drifting spiral waves of excitation in isolated cardiac muscle. Nature. 355(6358): 349-351.
4. Zhabotinskii AM. (1975);Sele-wave processes in distributed systems with diffusion coupling. Radiophysics and Quantum Electronics. 17(4): 448-452.
5. Arecchi F T, Meucci R and Gadomski W 1987 Phys. Rev. Lett. 58 2205
6. Hennequin D, de Tomasi F, Zambon B and Arimondo E 1988 Phys. Rev. A 37 2243
7. Karam F. F., Kadhim M. I., and Alkaim A. F. . (2015);Optimal conditions for synthesis of 1, 4-naphthaquinone by photocatalytic oxidation of naphthalene in closed system reactor. Int. J. Chem. Sci. 13(2): 650-660.
8. A. F. Alkaim, A.M. Aljeboree, N.A. Alrazaq, S.J. baqir, F.H. hussein, and A.J. lilo. (2014);Effect of pH on Adsorption and Photocatalytic Degradation Efficiency of Different Catalysts on Removal of Methylene Blue. Asian Journal of Chemistry. 26(24): 8445-8448.
9. Giacomelli G, Calzavara M, Arecchi FT (1989) Instabilities in a semiconductor laser with delayed optoelectronic feedback. Opt Commun 74:97-101
10. Loiko NA, Samson AM (1992) Possible regimes of generation of a semiconductor laser with a delayed optoelectronic feedback. Opt Commun 93:66-72

11. Lee EK, Pang HS, Park JD, Lee H (1993) Bistability and chaos in an injectionlocked semiconductor laser. *Phys Rev A* 47:736–739
12. F. Marino, M. Ciszak, S. F. Abdalah, K. Al-Naimee, R. Meucci, and F. T. Arecchi, *PHY. REV. E* 84, 047201, 2011
13. M. Bertram and A. S. Mikhailov, *Phys. Rev. E* 63, 066102, 2001.
14. K. Al-Naimee, F. Marino, M. Ciszak, S.F. Abdalah, R. Meucci and F.T. Arecchi, “Excitability of periodic and chaotic attractors in semiconductor lasers with optoelectronic feedback,” *Eur. Phys. J. D* 58, 187–189, 2010.
15. Bjorn Globisch, Christian Otto, Eckehard Scholl and Kathy Ludge, “Influence of carrier lifetimes on the dynamical behavior of quantum-dot lasers subject to optical feedback,” FIE09 dated July 24, 2012.
16. Geertje Hek, Vivi Rottshafer, “semiconductor laser with filtered optical feedback: bridge between conventional feedback and optical injection, ” ENOC-2005, Eindhoven, Netherlands, 7-12 August 2005.
